Paracyclophanes

Deutsche Ausgabe: DOI: 10.1002/ange.201411510
Internationale Ausgabe: DOI: 10.1002/anie.201411510

Cyclophanes Containing Bowl-Shaped Aromatic Chromophores: Three Isomers of *anti*-[2.2](1,4)Subphthalocyaninophane**

*Quan Liu, Soji Shimizu, and Nagao Kobayashi**

Abstract: *The connection of bowl-shaped aromatic boron subphthalocyanines with anti-[2.2]paracyclophane resulted in the first observation of electronic communication between convex and concave surfaces. Three isomers of anti-[2.2]-(1,4)subphthalocyaninophane, described as concave–concave (**CC**), convex–concave (**CV**), and convex–convex (**VV**) according to the orientation of the subphthalocyanine units, were synthesized and characterized by various spectroscopic techniques, including ^{1}H NMR, electronic absorption, fluorescence, and magnetic circular dichroism spectroscopy and X-ray crystallography, together with molecular-orbital calculations. On going from the **CC** system to **CV** and further to **VV**, the Q band broadened and finally split as a result of through-space expansion of the conjugated systems, which were also reproduced theoretically.*

When two or more aromatic chromophores come within close proximity, they show electronic communication that can be readily detected by electronic absorption and/or fluorescence spectroscopy. In particular, cofacially arranged aromatic molecules exhibit absorption spectra that differ significantly from those of the constituent monomeric molecules. In this respect, [2.2]paracyclophane, in which the *para* positions of the two benzene molecules are linked by two ethylene bridges, is well-known and has attracted the interest of many researchers for more than 60 years since its discovery around 1950.[1] Subsequently, similar cyclophanes consisting of naphthalene,[2] pyrene, anthracene, purine, and even porphyrins of various spacing and orientations have been synthesized in attempts to elucidate or understand the transannular interaction, that is, the electronic communication required, for example, for the design of organic materials for applications in optoelectronic technologies and catalysis.[3] Owing to the small distance between the two constituent benzene units, paracyclophane is generally considered to be one of the most suitable cyclophanes for investigating the transannular interaction. To our knowledge, all previously reported cyclophane derivatives containing aromatic chromophores consist of flat π-conjugated molecules, and no species consisting of curved aromatic molecules has been described. However, as demonstrated by intensive studies on fullerenes,[4] carbon nanotubes,[5] and their fragment molecules, such as corannulene[6] and sumanenes,[7] curved molecules are also important for the elucidation of the inherent properties of π-conjugated systems.

Herein, we report the synthesis and characterization of [2.2]paracyclophane derivatives containing two bowl-shaped aromatic boron subphthalocyanines (SubPcs), which are contracted analogues of phthalocyanines that contain three isoindole rings.[8,9] The combination of two SubPc units with [2.2]paracyclophane produces three isomers, which differ in the orientation of the convex and concave surfaces of the SubPc units with respect to the paracyclophane moiety. The difference in the electronic communication between the curved conjugated systems through the cyclophane moiety can be detected as changes in spectroscopic properties. These differences in the structure and properties of [2.2]paracyclophane derivatives with curved chromophores are described herein.

anti-[2.2](1,4)Subphthalocyaninophane and its monomer species, *anti*-[2.2](3,6)phthalonitrilosubphthalocyaninophane, were synthesized by simply treating 4,5,12,13-tetracyano-[2.2]paracyclophane[10] with an excess of tetrafluorophthalonitrile in the presence of boron trichloride in *p*-xylene at reflux (Scheme 1). The crude product was treated with an excess of phenol to prevent adsorption and axial-ligand substitution during purification by silica-gel column chromatography. As expected, as a result of the bowl shape of SubPc, three isomers of *anti*-[2.2](1,4)subphthalocyaninophane (concave–concave (**CC**), convex–concave (**CV**), and convex–convex (**VV**) isomers) and two isomers of its monomer species (*endo* (**endo**) and *exo* (**exo**) isomers) were obtained, along with perfluorinated SubPc as the major product. The yields of the dimer species were 2.2% for **CC**, 4.8% for **CV**, and 15.7% for **VV**, and those of the monomer species were 1.5% for **endo** and 5.1% for **exo**. The higher yields of **VV** and **exo** as compared to those of **CC** and **endo** are indicative of preferential formation of the sterically less hindered compounds with the adjacent moiety residing on the *exo* side of the SubPc unit.

The crystal structures of **CC** and **VV** were elucidated by X-ray crystallographic analysis of single crystals obtained by the slow diffusion of hexane into solutions of these dimer

[*] Dr. Q. Liu, Prof. N. Kobayashi
Department of Chemistry
Graduate School of Science, Tohoku University
Sendai 980-8578 (Japan)
E-mail: nagok@m.tohoku.ac.jp
Prof. S. Shimizu
Department of Chemistry and Biochemistry
Graduate School of Engineering, Kyushu University
Fukuoka 819-0395 (Japan)

[**] This research was partly supported by Grants-in-Aid for Scientific Research on Innovative Areas (25109502, "Stimuli-Responsive Chemical Species") and Scientific Research (B; No. 23350095) from the Ministry of Education, Culture, Sports, Science, and Technology (MEXT). We thank Prof. Takeaki Iwamoto and Dr. Shintaro Ishida (Tohoku University) for X-ray crystallographic measurements.

Supporting information for this article is available on the WWW under http://dx.doi.org/10.1002/anie.201411510.

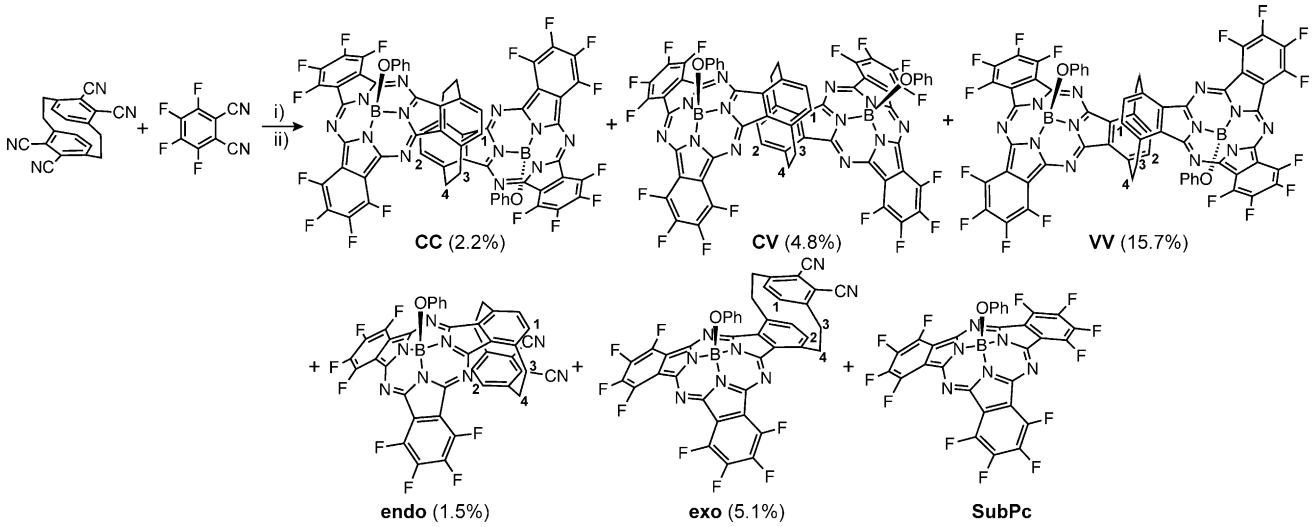

Scheme 1. Synthesis of *anti*-[2.2](1,4)subphthalocyaninophane and *anti*-[2.2](3,6)phthalonitrilosubphthalocyaninophane. Reaction conditions: i) BCl_3, *p*-xylene, reflux; ii) phenol, 125 °C.

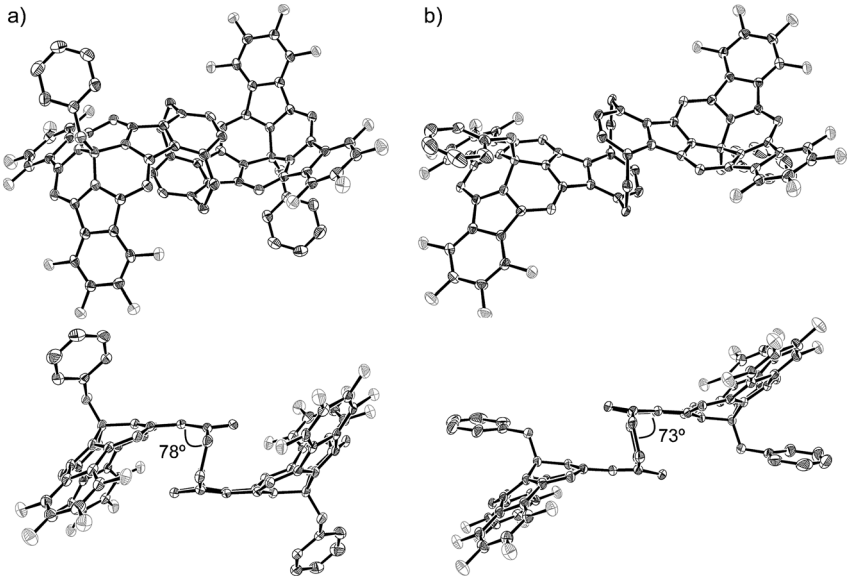

Figure 1. X-ray crystal structures of a) **CC** and b) **VV** (top: top view, bottom: side view). The thermal ellipsoids were scaled to the 50% probability level. Hydrogen atoms were omitted for clarity.

species in $CHCl_3$.[11] It was found that the SubPc units each reside on the *endo* and *exo* surface of the other SubPc unit in **CC** and **VV**, respectively (Figure 1). A boron atom lies above the plane defined by the three coordinating nitrogen atoms by 0.64 Å in **CC** and 0.63 Å in **VV**; these distances are within the range observed for regular SubPcs (0.59–0.66 Å).[9b,c] The distance between the bridge-head carbon atoms is 2.75 Å for **CC** and 2.76 Å for **VV**. Owing to the short distance of the ethylene bridge, the two bridged benzene rings are deformed, and have shallow V-shaped structures. The distance between the mean planes of the cyclophane benzene rings is 2.98 Å for **CC** and 2.91 Å for **VV**. The dihedral angle between these mean planes and the mean plane of the four ethylene carbon atoms is 78° for **CC** and 73° for **VV** (Figure 1). These angles indicate that the cyclophane unit adopts a slip-stacked conformation, which is in clear contrast to the perpendicular orientation of the two planes in the parent [2.2]paracyclophane.[12] Although we could not obtain a suitable single crystal for structural analysis, the remaining dimer species was assigned as the convex–concave isomer (**CV**). Its structure was supported by ^{1}H NMR spectroscopy.

In the ^{1}H NMR spectra, the chemical shifts of the cyclophane hydrogen atoms unambiguously reflect the structural features of these cyclophane-containing SubPcs (Figure 2). With respect to the benzene hydrogen atoms of unsubstituted [2.2]paracyclophane at 6.48 ppm,[1,3] those of **CC** exhibited a significant upfield shift by 3.92 ppm to 2.54 ppm, whereas the upfield shift observed for **VV** was marginal, at only 0.03 ppm. Owing to their presence on both the *endo* and *exo* sides, the signals of the cyclophane hydrogen atoms appeared at 6.48 and 2.38 ppm in the case of **CV**. On the basis of this assignment, the monomer species **endo** and **exo**, which exhibited a proton signal at 2.32 and 6.09 ppm, respectively, could be assigned as the *endo* and *exo* isomers. These experimental chemical shifts were reproduced well by DFT calculations (see Figure S1 in the Supporting Information). The cyclophane bridging also affected the chemical shifts of the axial phenoxy ligand. The downfield shifts observed for the axial ligand on the SubPc unit with *exo* bridging can be explained by the deshielding effect of the diatropic ring current of the benzene ring or the subphthalocyanine moiety on the *exo* side.

Despite the difference in the distance from the center of the SubPc unit, the clear upfield shift of the *endo* cyclophane

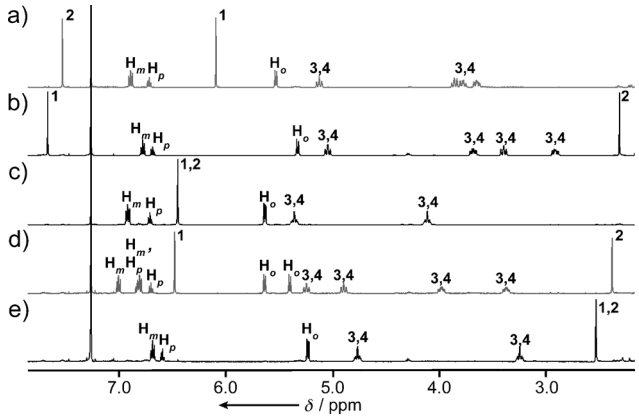

Figure 2. ^{1}H NMR spectra of a) **exo**, b) **endo**, c) **VV**, d) **CV**, and e) **CC** in $CDCl_3$. The assignment follows the numbering scheme in Scheme 1. $\mathbf{H}_o$, $\mathbf{H}_m$, and $\mathbf{H}_p$ denote hydrogen atoms at the *ortho*, *meta*, and *para* positions of the axial phenyl substituents.

hydrogen atoms indicated a more significant shielding effect of the diatropic ring current on the *endo* side than on the *exo* side. Such an effect was also suggested by Torres and co-workers and by us upon comparison of the chemical shifts of hydrogen atoms residing on the *endo* and *exo* sides of the SubPc units in the pentamethylcyclopentadienylruthenium complex of SubPcs[13] and a core-modified SubPc analogue.[14] However, dynamic molecular motions of the probing moieties are inherent to these systems, such as rotation of the Cp* ligand. The current cyclophane-containing SubPc systems are the first structurally rigid probes for the diatropic ring-current effect arising from the bowl-shaped aromatic molecules.

UV/Vis absorption and magnetic circular dichroism (MCD) spectroscopic measurements revealed the extent of the perturbation by annulation of the cyclophane unit and the through-space interaction based on the transannular effect.[15] In comparison with regular SubPcs, the dimer species showed dramatic spectral changes on going from **CC** to **CV** and to **VV** (Figure 3 a–c). The Q-band spectral shape of **CC** was similar to those of regular SubPcs with only a redshift by approximately 20 nm. Without any change in the Q-band position, **CV** and **VV** exhibited broadening and a decrease in intensity of the Q band, and in the case of **VV**, the Q-band absorption split into two peaks at 617 and 593 nm. Because the molecular symmetries of these SubPcs are lower than C_3, all of the MCD spectra in the Q-band region consist of a superimposition of Faraday *B* terms with a minus-to-plus sequence on ascending energy, which resulted in pseudo Faraday *A* terms, except for **VV**.[16,17] Owing to the splitting of the Q band, **VV** exhibited clear *B* terms at 608 and 585 nm. In contrast to the dependence of the absorption spectral morphologies on the manner of bridging of the two SubPc units in the case of the dimers, both of the monomer species, **exo** and **endo**, exhibited similar absorption and MCD spectra with respect to those of regular SubPcs, although the Q band was slightly shifted to the red by approximately 15 nm (Figure 3 d,e). All compounds retained the fluorescence properties of SubPc analogues[9] and exhibited intense emission with fluorescence quantum yields of 0.15 for **CC** and 0.16 for both **CV** and **VV**. The redshift in fluorescence was of the order observed for the absorption

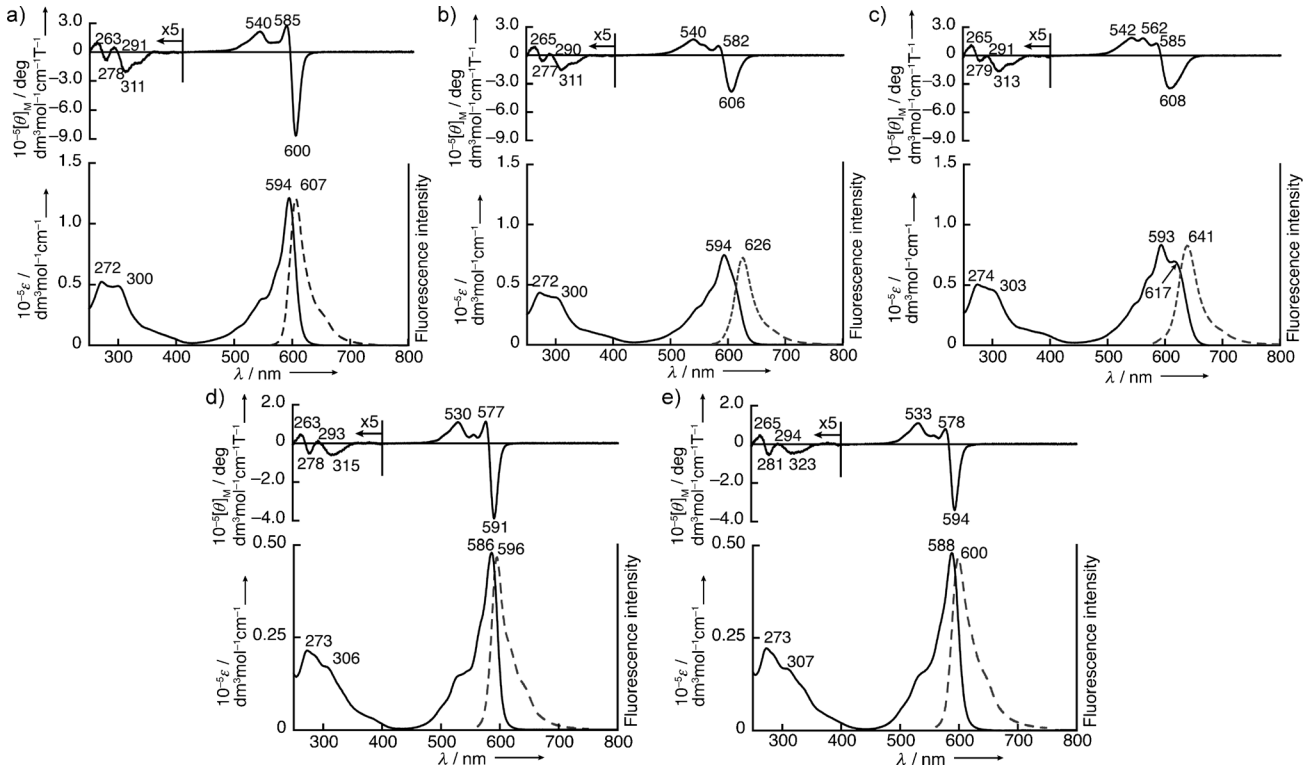

Figure 3. UV/Vis absorption (bottom, solid line), MCD (top), and fluorescence spectra (bottom, dashed line) of a) **CC**, b) **CV**, c) **VV**, d) **endo**, and e) **exo** in $CHCl_3$.

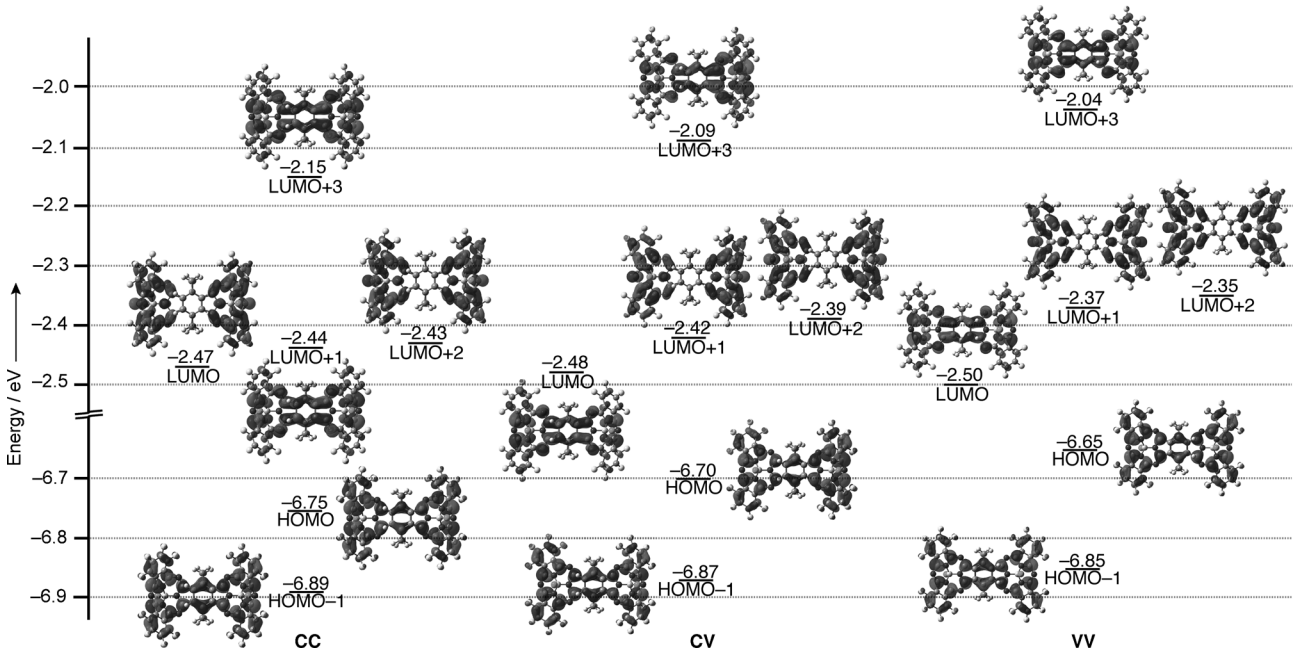

Figure 4. Partial MO diagrams derived from CAM-B3LYP/6-31G(d) level DFT calculations of *anti*-[2.2](1,4)subphthalocyaninophane **CC** (left), **CV** (middle), and **VV** (right).

spectra (**endo**: 596 nm, **exo**: 600 nm, **CC**: 607 nm, **CV**: 626 nm, **VV**: 641 nm).

To enhance our understanding of the perturbation caused by the annulation of the cyclophane unit for the monomer species and the cyclophane bridging for the dimer species, DFT and time-dependent (TD) DFT calculations were carried out at the CAM-B3LYP/6-31G(d)[18] level by using model structures, in which the axial phenoxy ligands were replaced with chlorine atoms for simplicity. For comparison, a half structure of the dimer species (**M1**; see Figure S2), in which two methylene substituents are replaced with two methyl substituents, was also calculated. The TDDFT calculations estimated that the Q bands mainly consist of transitions between the six frontier molecular orbitals (MOs), the HOMO-1 and HOMO, and the LUMO–LUMO + 3, which are ascribed to products of linear combinations of the HOMO and the LUMO and LUMO + 1 of **M1** (Figure 4; see also Table S1 in the Supporting Information). In the case of the homo- and heterodimer systems of Pc, SubPc, and related analogues sharing π-conjugated aromatic rings, such as benzene, naphthalene, and anthracene,[19–24] the frontier MOs are known to be similarly developed by linear combination of the frontier MOs of the corresponding monomer species. In this respect, the through-space expansion of the conjugated systems through the cyclophane bridge in the case of the current SubPc dimer species was supported in theory. In fact, a certain amount of the MO coefficient was observed between the benzene rings of the cyclophane unit for the LUMO + 1 of **CC** and the LUMO of **CV** and **VV** (see Figures S3–S5).

The TDDFT calculations reproduced well the observed redshift and broadening/splitting of the Q band on going from **CC** to **CV** and further to **VV** (see Table S1). Considering that the transition dipole moment of the lower-energy theoretical Q band lies along the long axis of the molecule, it can be concluded that changes in the molecular size and hence the size of the conjugated system along this axis in the order from **CC** to **CV** and to **VV** are related to the observed redshift of this band (see Figure S6). This kind of conclusion could be reached in this study for the first time by the preparation of cyclophane derivatives containing curved conjugated systems. Although the change in the Q-band position of the monomer species was very small (**endo**: 586 nm, **exo**: 588 nm), it can similarly be explained by a slight elongation of the conjugated system along the long molecular axis from **endo** to **exo**.

In summary, we have succeeded in designing, synthesizing, and separating three isomers of *anti*-[2.2]-(1,4)subphthalocyaninophane and two isomers of *anti*-[2.2]-(3,6)phthalonitrilosubphthalocyaninophane, in which the transannular interaction between the two bowl-shaped π-conjugated systems was investigated. The ^{1}H NMR spectra of these compounds unambiguously unveiled completely different environments on the *endo* and *exo* sides of the SubPc units. The broadening, redshift, and splitting observed in the Q band region of the absorption spectra of these compounds were reproduced well and explained by theoretical calculations. This study provides a new approach for understanding through-space electronic communication between chromophores.

Keywords: cyclophanes · ring-current effects · subphthalocyanines · transannular interactions · π conjugation

How to cite: *Angew. Chem. Int. Ed.* **2015**, *54*, 5187–5191
Angew. Chem. **2015**, *127*, 5276–5280

[1] a) D. J. Cram, H. Steinberg, *J. Am. Chem. Soc.* **1951**, *73*, 5691–5704; b) C. J. Brown, A. C. Farthing, *Nature* **1949**, *164*, 915–916.

[2] H. H. Wasserman, P. M. Keehn, *J. Am. Chem. Soc.* **1969**, *91*, 2374 – 2375.
[3] a) F. Diederich, *Cyclophanes*, RSC, Cambridge, **1991**; b) R. Gleiter, H. Hopf, *Modern Cyclophane Chemistry*, Wiley-VCH, Weinheim, **2004**.
[4] a) M. S. Dresselhaus, G. Dresselhaus, P. Eklund, *Science of Fullerenes and Carbon Nanotubes: Their Properties and Applications*, Academic Press, San Diego, **1996**; b) F. Langa, F. Nierengarten, *Fullerenes: Principles and Applications*, 2nd ed., RSC, London, **2012**; c) K. Kadish, R. S. Ruoff, *Fullerenes: Chemistry, Physics, and Technology*, Wiley, New York, **2000**.
[5] a) M. J. O'Connel, *Carbon Nanotubes*, CRC, Boca Raton, **2012**; b) S. Reich, C. Thomsen, J. Maultzsch, *Carbon Nanotubes: Basic Concepts and Physical Properties*, Wiley-VCH, Weinheim, **2004**.
[6] a) V. M. Tsefrikas, L. T. Scott, *Chem. Rev.* **2006**, *106*, 4868 – 4884; b) Y. T. Wu, J. S. Siegel, *Chem. Rev.* **2006**, *106*, 4843 – 4867.
[7] a) H. Sakurai, T. Daiko, T. Hirao, *Science* **2003**, *301*, 1878; b) T. Amaya, T. Hirao, *Chem. Commun.* **2011**, *47*, 10524 – 10535.
[8] A. Meller, A. Ossko, *Monatsh. Chem.* **1972**, *103*, 150 – 155.
[9] a) "Synthesis and Spectroscopic Properties of Phthalocyanine Analogues": N. Kobayashi in *The Porphyrin Handbook*, *Vol. 15* (Eds.: K. M. Kadish, K. M. Smith, R. Guilard), Academic Press, San Diego, **2003**, chap. 100, pp. 161 – 262; b) C. G. Claessens, D. González-Rodríguez, T. Torres, *Chem. Rev.* **2002**, *102*, 835 – 853; c) C. G. Claessens, D. González-Rodríguez, M. S. Rodríguez-Morgade, A. Medina, T. Torres, *Chem. Rev.* **2014**, *114*, 2192 – 2277.
[10] Y. Asano, A. Muranaka, A. Fukasawa, T. Hatano, M. Uchiyama, N. Kobayashi, *J. Am. Chem. Soc.* **2007**, *129*, 4516 – 4517.
[11] Crystallographic data for **CC**: $C_{64}H_{22}N_{12}F_{16}B_2O_2$, MW = 1316.55, triclinic, space group $P\bar{1}$ (no. 2), $a = 12.985(3)$, $b = 13.407(3)$, $c = 18.072(4)$ Å, $\alpha = 105.973(2)$, $\beta = 99.477(2)$, $\gamma = 94.994(2)°$, $V = 2954.2(10)$ Å^3, $Z = 2$, $\rho_{calcd} = 1.480$ g cm^{-3}, $T = -173(2)°$C, 27405 measured reflections, 8088 unique reflections ($R_{int} = 0.0279$), $R = 0.0557$ ($I > 2\sigma(I)$), $R_w = 0.1477$ (all data), goodness-of-fit on F_2: 1.071, largest diff. peak/hole: 0.483 and -0.298 e Å^{-3}; crystallographic data for **VV**: $C_{64}H_{22}N_{12}F_{16}B_2O_2$, MW = 1316.55, monoclinic, space group $P2_1/n$ (no. 14), $a = 11.751(2)$, $b = 22.522(4)$, $c = 25.299(4)$ Å, $\beta = 93.888(2)°$, $V = 6679.9(19)$ Å^3, $Z = 4$, $\rho_{calcd} = 1.309$ g cm^{-3}, $T = -173(2)°$C, 62905 measured reflections, 9840 unique reflections ($R_{int} = 0.0492$), $R = 0.0405$ ($I > 2\sigma(I)$), $R_w = 0.1170$ (all data), goodness-of-fit on F_2: 1.048, largest diff. peak/hole: 0.305 and -0.366 e Å^{-3}. CCDC 1033205 (**CC**) and 1033340 (**VV**) contain the supplementary crystallographic data for this paper. These data can be obtained free of charge from The Cambridge Crystallographic Data Centre via www.ccdc.cam.ac.uk/data_request/cif.
[12] H. Hope, K. N. Truebloo, J. Bernstein, *Acta Crystallogr. Sect. B* **1972**, *28*, 1733 – 1743.
[13] E. Caballero, J. Fernandez-Ariza, V. M. Lynch, C. Romero-Nieto, M. S. Rodríguez-Morgade, J. L. Sessler, D. M. Guldi, T. Torres, *Angew. Chem. Int. Ed.* **2012**, *51*, 11337 – 11342; *Angew. Chem.* **2012**, *124*, 11499 – 11504.
[14] S. Shimizu, S. Nakano, A. Kojima, N. Kobayashi, *Angew. Chem. Int. Ed.* **2014**, *53*, 2408 – 2412; *Angew. Chem.* **2014**, *126*, 2440 – 2444.
[15] a) J. N. Moorthy, S. Mandal, A. Kumar, *New J. Chem.* **2013**, *37*, 82 – 88; b) G. P. Bartholomew, G. C. Bazan, *Acc. Chem. Res.* **2001**, *34*, 30 – 39; c) H. Hinrichs, A. J. Boydston, P. G. Jones, K. Hess, R. Herges, M. M. Haley, H. Hopf, *Chem. Eur. J.* **2006**, *12*, 7103 – 7115; d) G. C. Bazan, *J. Org. Chem.* **2007**, *72*, 8615 – 8635.
[16] a) J. Michl, *J. Am. Chem. Soc.* **1978**, *100*, 6801 – 6811; b) J. Michl, *Pure Appl. Chem.* **1980**, *52*, 1549 – 1563; c) J. Mack, M. J. Stillman, N. Kobayashi, *Coord. Chem. Rev.* **2007**, *251*, 429 – 453.
[17] a) A. Kaito, T. Nozawa, T. Yamamoto, M. Hatano, Y. Orii, *Chem. Phys. Lett.* **1977**, *52*, 154 – 160; b) A. Tajiri, J. Winkler, *Z. Naturforsch. A* **1983**, *38*, 1263 – 1269.
[18] Although the transition energies were slightly overestimated, use of the long-range corrected CAM-B3LYP exchange-correlation functional for the TDDFT calculations reproduced well the splitting of the Q band on going from **CC** to **CV** and further to **VV**: T. Yanai, D. P. Tew, N. C. Handy, *Chem. Phys. Lett.* **2004**, *393*, 51 – 57.
[19] N. Kobayashi, H. Lam, W. A. Nevin, P. Janda, C. C. Leznoff, T. Koyama, A. Monden, H. Shirai, *J. Am. Chem. Soc.* **1994**, *116*, 879 – 890.
[20] N. Shibata, S. Mori, M. Hayashi, M. Ueda, E. Tokunaga, M. Shiro, H. Sato, T. Hoshi, N. Kobayashi, *Chem. Commun.* **2014**, *50*, 3040 – 3043.
[21] J. Mack, X. Liang, T. V. Dubinina, J. G. Tomilova, T. Nyokong, N. Kobayashi, *J. Porphyrins Phthalocyanines* **2013**, *17*, 489 – 500.
[22] Y. Asano, J. Sato, T. Furuyama, N. Kobayashi, *Chem. Commun.* **2012**, *48*, 4365 – 4367.
[23] N. Kobayashi, H. Ogata, *Eur. J. Inorg. Chem.* **2004**, 906 – 914.
[24] N. Kobayashi, S. Nakajima, H. Ogata, T. Fukuda, *Chem. Eur. J.* **2004**, *10*, 6294 – 6312.

Received: November 28, 2014
Revised: January 29, 2015
Published online: February 25, 2015

